

Epitaxial Graphene Devices for Scanning Probe Measurements

Andrea Iagallo¹, Shinichi Tanabe², Stefano Roddaro¹, Makoto Takamura², Yoshiaki Sekine², Hiroki Hibino², Vaidotas Miseikis³, Camilla Coletti³, Vincenzo Piazza³, Fabio Beltram¹, and Stefan Heun¹

¹NEST, Istituto Nanoscienze–CNR and Scuola Normale Superiore
Piazza San Silvestro 12, 56127 Pisa, Italy

Phone: +39-050-509119, E-mail: andrea.iagallo@sns.it

²NTT Basic Research Laboratories, NTT Corporation

3-1 Morinosato Wakamiya, Atsugi, Kanagawa 243-0198, Japan

³Center for Nanotechnology Innovation @ NEST, Istituto Italiano di Tecnologia
Piazza San Silvestro 12, 56127 Pisa, Italy

Abstract

The magnetotransport properties of epitaxial graphene on SiC substrates play a central role in the development of monolithic technology for high quality graphene-based devices. Magnetotransport investigations in both the small field and the quantum Hall regime give valuable information on the disorder properties of the monolayer film and on the role of bilayer inclusions. In the small field region, we find an unexpected dependence of the intra-valley scattering and electron-electron interactions on carrier density in monolayer devices. In the quantum Hall regime, bilayer stripes shunting the devices are responsible for anomalies in the observed characteristics, which we explain in terms of a Landauer-Büttiker model.

1. Introduction

Recent years have seen the affirmation of scanning probe investigation techniques as powerful tools to investigate a great variety of transport phenomena in condensed matter physics. Among these techniques, scanning gate microscopy (SGM) has already been used to probe disorder potential [1-3], the properties of fractional and integer edge states in the quantum Hall regime [4-5], and for the spectroscopy of quantum dots [6-10]. In SGM measurements, the conductive tip of an atomic force microscope is used to induce a local electrostatic perturbation of the device properties while recording the global response of the system.

Graphene is a very appealing candidate for SGM experiments, because it displays a high mobility and surface conduction, thus allowing operation of the SGM in very close proximity to the device. In particular, epitaxial growth of graphene on SiC is one of the routes pursued in the quest for monolithic integration of graphene, and has reached high mobility and uniformity on the wafer scale [11]. In this form, graphene can be used for large scale fabrication of devices. Recently, the availability of a suitable dielectric [12] made it possible to perform top-gating of the graphene layer, thus making SiC-based devices ideal for SGM experiments. In the following, we describe the development

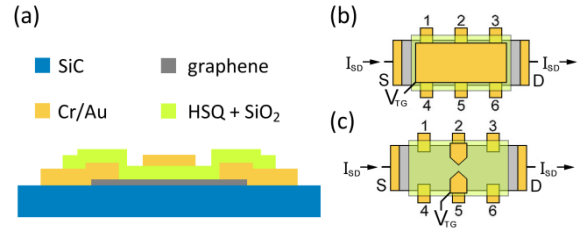


Fig. 1: (a) Section of the devices investigated and different top-gate layouts: (b) large-area top-gate and (c) split-gates.

and characterization of graphene-based devices for SGM experiments aimed to achieve local control of the filling factor in the quantum Hall regime.

2. Experimental work

Figure 1(a) shows a sketch of the devices analyzed in this work, consisting of large-area graphene Hall bars (length \times width = $300 \mu\text{m} \times 50 \mu\text{m}$) fabricated by standard optical lithography from an epitaxial graphene layer grown on a SiC(0001) wafer. Metallic contacts (Cr/Au, 5/250 nm) and a dielectric layer (140 nm of hydrogen silsequioxane (HSQ) and 40 nm of SiO₂) are further deposited. Finally, Cr/Au (10/180 nm) top gates were defined by e-beam lithography. We investigated two devices, in which the top-gate has either the form of a large-area top-gate (Fig. 1(b)) or a split-gate geometry (Fig. 1(c)).

Quantum Interference

In high quality graphene, the low density of short-range scatterers allows the Berry phase to manifest as a weak antilocalization (WAL) dip in the magnetoresistance [13]. As the π -phase contribution is averaged out by chirality-breaking scattering, enhanced backscattering results in a weak localization (WL) correction. Essential in driving the transition between WAL and WL regimes is the possibility of tuning the charge density in the graphene monolayer, which limited so far an exhaustive investigation of the interplay between localization and chirality for EG grown on SiC(0001).

We performed a systematic study of the quantum cor-

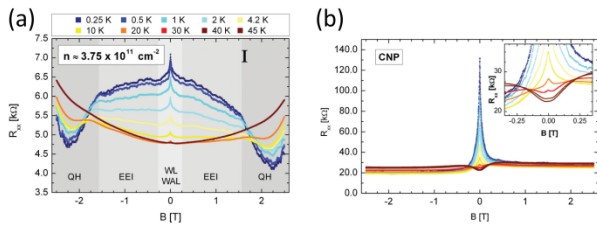


Fig. 2: Longitudinal resistance of the device in Fig. 1(b) for two values of the carrier density, $3.75 \times 10^{11} \text{ cm}^{-2}$ in (a) and close to the charge neutrality point (CNP) in (b), and at different temperatures.

rections to the magnetoresistance due to quantum interference of quasiparticles and electron-electron interaction on a top-gated device outlined in Fig. 1(b) [14]. Typical magnetotransport measurements as a function of temperature are shown in Figs. 2(a) and (b) for two different carrier densities. The measurements show distinctive features of W(A)L and electron-electron interaction, which were analyzed in the $-2.0 \times 10^{10} \text{ cm}^{-2}$ to $3.75 \times 10^{11} \text{ cm}^{-2}$ density region and in the 0.25 K to 45 K temperature range to extract the behavior of the *inter*- and *intra*-valley scattering times. Our results highlight a dependence of the *intra*-valley scattering on carrier density not ascribable to the sole warping of the Dirac cone. The electron-electron interaction was also found to depend on the carrier density, a fact not accounted for by present theory.

Quantum Hall regime

The second device design, shown in Fig. 1(c), is aimed at performing local tuning of the filling factor by the SGM tip. Measurements in the quantum Hall regime show a departure from the quantized resistance values expected for ideal monolayer graphene, in contrast to what was observed for the top-gated device used for the characterization of interference properties. In particular, at quantizing magnetic field, the longitudinal resistance assumes unexpectedly large values $R_{xx} \approx 10 \text{ k}\Omega$, while the transversal resistance shows much lower values $R_{xy} \approx 2 \text{ k}\Omega$. The most striking feature is that the magnetoresistance curves display peculiar symmetry properties, as shown in Figs. 3(a) and (b). Bilayer inclusions forming at the SiC atomic steps are believed to be responsible for the observed behavior. As supported by Raman maps of the device shown in Fig. 3(c), the step terraces of the SiC substrate were oriented perpendicularly to the Hall bar, and so long continuous bilayer stripes are present, which can cause shunting of the edge states at opposite sides of the bar. A simple model based on the Landauer-Büttiker formalism (see Fig. 3(d)) succeeds in explaining the observed transport anomalies.

3. Conclusions

We present a comprehensive investigation of the magnetotransport properties of epitaxial graphene devices and find a significant influence of the charge density on the intravalley scattering time. Furthermore, we observe a modulation of the electron-electron interaction with charge

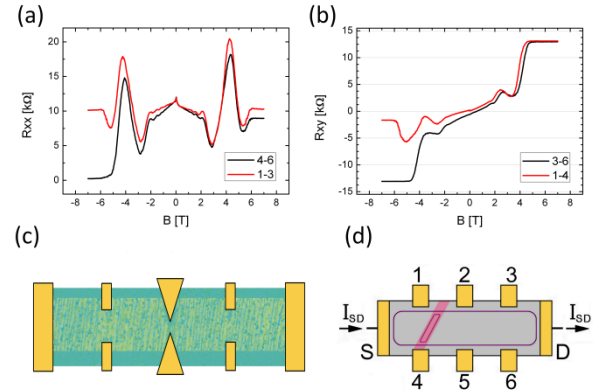


Fig. 3: Quantum Hall traces in a split-gate device containing graphene bilayer shunts: a) longitudinal and b) transversal resistance. c) Raman map of the device showing monolayer (light green) and bilayer (dark) graphene regions. The outline of the contacts and gates is superimposed. d) Schematic of edge state arrangement for a bilayer inclusion.

density not accounted for by present theory. The measurements in the quantum Hall regime allow to shed light on the role of bilayer strips on the transport properties of epitaxial graphene on SiC, an aspect which is essential in the development of an effective integration technology.

References

- [1] M. A. Topinka, B. J. LeRoy, R. M. Westervelt, S. E. J. Shaw, R. Fleischmann, E. J. Heller, K. D. Maranowski, and A. C. Gossard, *Nature* **410**, 183 (2001).
- [2] M. P. Jura, M. A. Topinka, L. Urban, A. Yazdani, H. Shtrikman, L. N. Pfeifer, K. W. West, and D. Goldhaber-Gordon, *Nat. Phys.* **3**, 841 (2007).
- [3] N. Paradiso, S. Heun, S. Roddaro, G. Biasiol, L. Sorba, D. Venturelli, F. Taddei, V. Giovannetti, and F. Beltram, *Phys. Rev. B* **86**, 085326 (2012).
- [4] N. Paradiso, S. Heun, S. Roddaro, L. Sorba, F. Beltram, G. Biasiol, L. N. Pfeiffer, and K. W. West, *Phys. Rev. Lett.* **108**, 246801 (2012).
- [5] N. Pascher, C. Rössler, T. Ihn, K. Ensslin, C. Reichl, and W. Wegscheider, *Phys. Rev. X* **4**, 011014 (2014).
- [6] M. T. Woodside and P. L. McEuen, *Science* **296**, 1098 (2002).
- [7] A. C. Bleszynski, F. A. Zwanenburg, R. M. Westervelt, A. L. Roest, E. P. A. M. Bakkers, and L. P. Kouwenhoven, *Nano Lett.* **7**, 2559 (2007).
- [8] P. Fallahi, A. C. Bleszynski, R. M. Westervelt, J. Huang, J. Walls, and E. J. Heller, *Nano Lett.* **5**, 223 (2005).
- [9] A. E. Gildemeister, T. Ihn, M. Sigrist, K. Ensslin, D. C. Driscoll, and A. C. Gossard, *Phys. Rev. B* **75**, 195338 (2007).
- [10] N. Aoki, R. Brunner, A. M. Burke, R. Akis, R. Meisels, D. K. Ferry, and Y. Ochiai, *Phys. Rev. Lett.* **108**, 136804 (2012).
- [11] S. Tanabe, Y. Sekine, H. Kageshima, M. Nagase, and H. Hibino, *Phys. Rev. B* **84**, 115458 (2011).
- [12] S. Tanabe, Y. Sekine, H. Kageshima, M. Nagase, and H. Hibino, *Appl. Phys. Express* **3**, 075102 (2010).
- [13] F. V. Tikhonenko, A. A. Kozikov, A. K. Savchenko, and R. V. Gorbachev, *Phys. Rev. Lett.* **103**, 226801 (2009).
- [14] A. Iagallo, S. Tanabe, S. Roddaro, M. Takamura, H. Hibino, and S. Heun, *Phys. Rev. B* **88**, 235406 (2013).